

**Supporting information for:**  
**Structure-Directed Exciton Dynamics in Templated**  
**Molecular Nanorings**

Juliane Q. Gong,<sup>\*,†</sup> Patrick Parkinson,<sup>†</sup> Dmitry V. Kondratiuk,<sup>‡</sup> Guzmán

Gil-Ramírez,<sup>‡</sup> Harry L. Anderson,<sup>‡</sup> and Laura M. Herz<sup>\*,†</sup>

*Department of Physics, University of Oxford, Clarendon Laboratory, Parks Road, Oxford*

*OX1 3PU, United Kingdom, and Department of Chemistry, University of Oxford,*

*Chemistry Research Laboratory, Oxford OX1 3TA, United Kingdom*

E-mail: juliane.gong@physics.ox.ac.uk; l.herz1@physics.ox.ac.uk

---

\*To whom correspondence should be addressed

<sup>†</sup>Oxford Physics

<sup>‡</sup>Oxford Chemistry

## Absorption and Emission Spectra

Figure S1 shows absorption and emission spectra at room temperature of all the porphyrin nanorings under investigation. Absorption spectra were measured over the range of 320 – 1100 nm and the emission spectra were measured in the range of 800 – 1200 nm at an excitation wavelength of 520 nm corresponding to the Soret band. The nanoring concentration in solution was on the order of  $10^{-4}$  mol/L and the absorbance at the Soret band was kept at approximately 0.2 for all samples.

**c-P10** and **c-P12** exhibit similar spectra, and a Stokes shift between absorption and emission peaks of about 50 nm. All templated rings show a sharpening in the features (compared to untemplated rings). The absorption peak are located around 860 nm, demonstrating a red shift of about 50 – 60 nm with respect to the untemplated rings. The Stokes shifts between absorption and emission peaks are about 40 nm and hence only slightly lowered through templating.

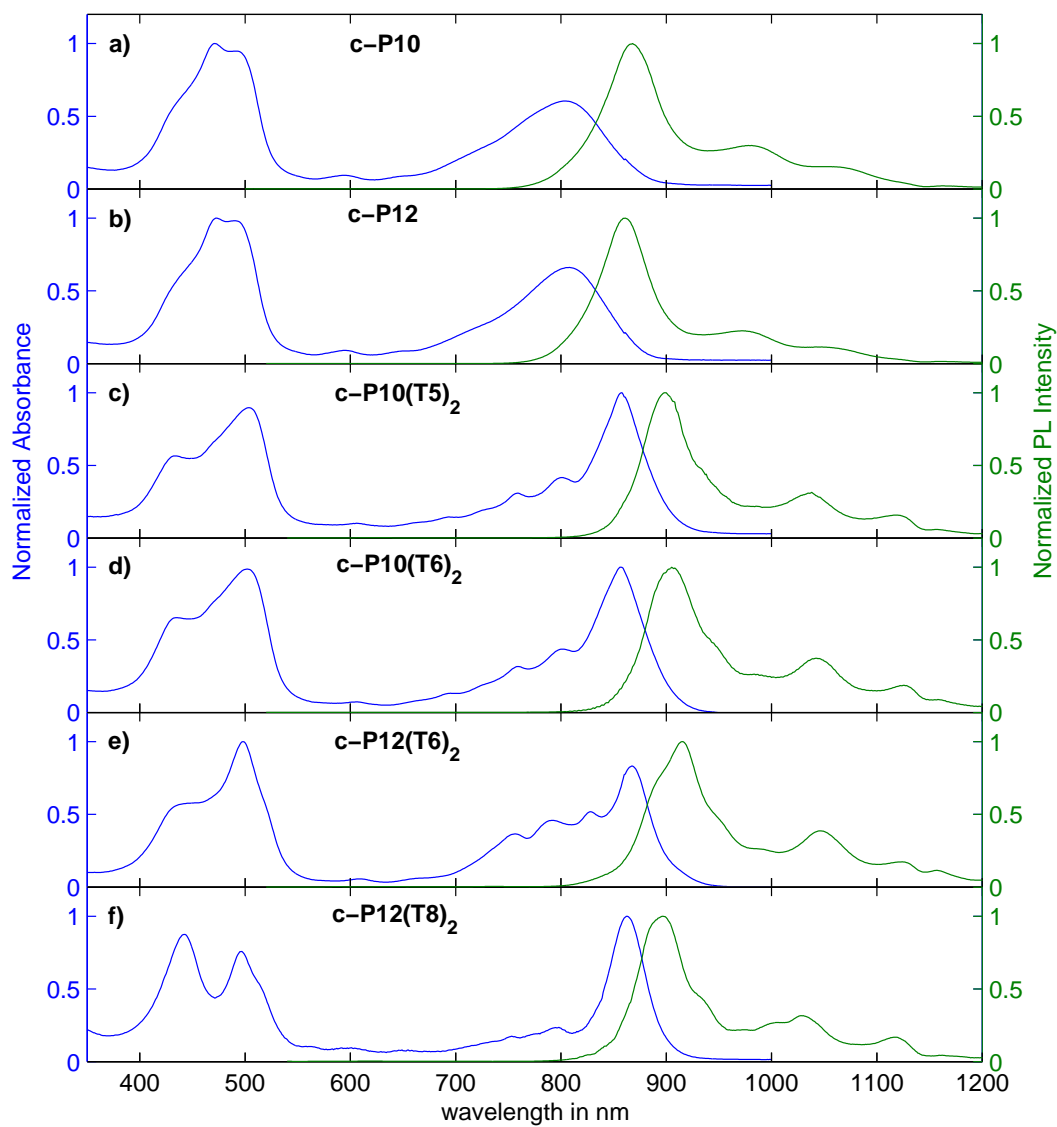


Figure S1: Normalized steady-state absorption (blue lines) and time-integrated photoluminescence (green lines) spectra at 295 K for (a) *c-P10* (b) *c-P12* in toluene/1% pyridine and (c) *c-P10*·(*T5*)<sub>2</sub>, (d) *c-P10*·(*T6*)<sub>2</sub>, (e) *c-P12*·(*T6*)<sub>2</sub> and (f) *c-P12*·(*T8*)<sub>2</sub> in toluene solution. The emission spectra were recorded after excitation at 520 nm (Soret band).

# Instrumental Response Function

Instrumental response functions (IRF) of the photoluminescence upconversion system were recorded using  $\text{TiO}_2$  in water as a scattering material held in a cuvette, with the excitation wavelength set to 780 nm and detecting the elastically scattered light at 780 nm, gated by the 780-nm gate pulse to give upconverted photons at 390 nm. Excitation occurred through the front of the cuvette with respect to the collection pathway, i.e. the scattered light was collected in back-scatter geometry, identical to the configuration used for the nanoring photoluminescence reported in the main article. If the excitation pulse was polarized perpendicular with respect to the detection pulse polarization, no upconverted signal could be detected, because the sample does not absorb light at this wavelength but only scatters. Therefore, the two excitation polarization settings of (i) parallel and (ii)  $70^\circ$  with respect to the detection pulse polarization were used to record the instrumental response functions, as illustrated in Figure S2.

Fitting to the IRF was carried out using a Gaussian model. From the fit to the data points, the centre of the peak and the full width at half maximum (FWHM) can be extracted. It is found that a temporal shift of 18 fs with a 50% error exists between the peak centres as a result of the walk-off effect in the Glen-Thompson polariser used to control the polarization of the excitation pulse. The actual temporal shift between the perpendicular and parallel polarized excitation pulses may be slightly (but insignificantly) larger. The FWHM of the Gaussian peaks are found to be 280 nm (7%) and 258 nm (13%) and hence the resolution limit of the upconversion system is about 270 nm.

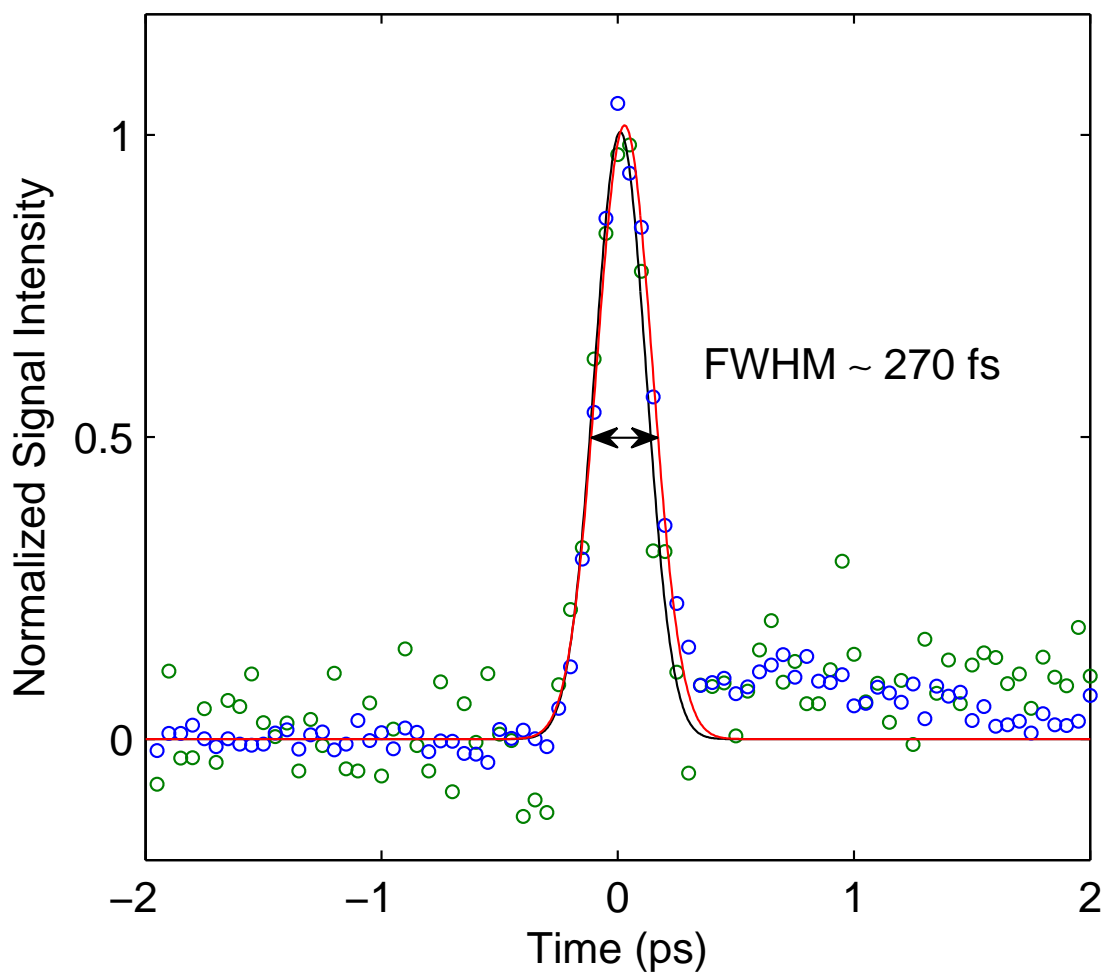


Figure S2: Normalized instrumental response function (IRF) of the photoluminescence up-conversion system, measured with excitation at 780 nm polarized parallel (blue) and almost perpendicular (green) to the detection pulse polarization. Fitting to these IRF data is carried out using a Gaussian function for both parallel (red) and almost perpendicularly (black) polarized excitation pulses. The full width at half maximum is similar in both cases (270 fs).

## PL Transients and Anisotropy Dynamics

Figure S3 depicts the two polarization components of the PL emission transients for all porphyrin rings investigated in this study, together with the derived PL anisotropy dynamics. The concentration of the sample solutions was on the order of  $10^{-4}$  mol/L. To achieve the best signal-to-noise ratio with the optimum filter combination in the PL upconversion set-up, the detection wavelengths were chosen around the emission peaks and the excitation wavelengths were slightly blue-shifted with respect to the absorption peak. Untemplated rings are excited at 780 nm and templated rings at 820 nm, as the latter demonstrate red-shifted spectra.

When computing the anisotropy dynamics, the temporal shift between the parallel and perpendicular polarized emission components with respect to the excitation pulse polarization (as described above) was taken into account. The onset of the PL emission at 0 ps is defined as the point when the PL signal size reaches half of its maximum value. The PL anisotropy is observed to be constant over time in the time window of 15 ps following excitation.

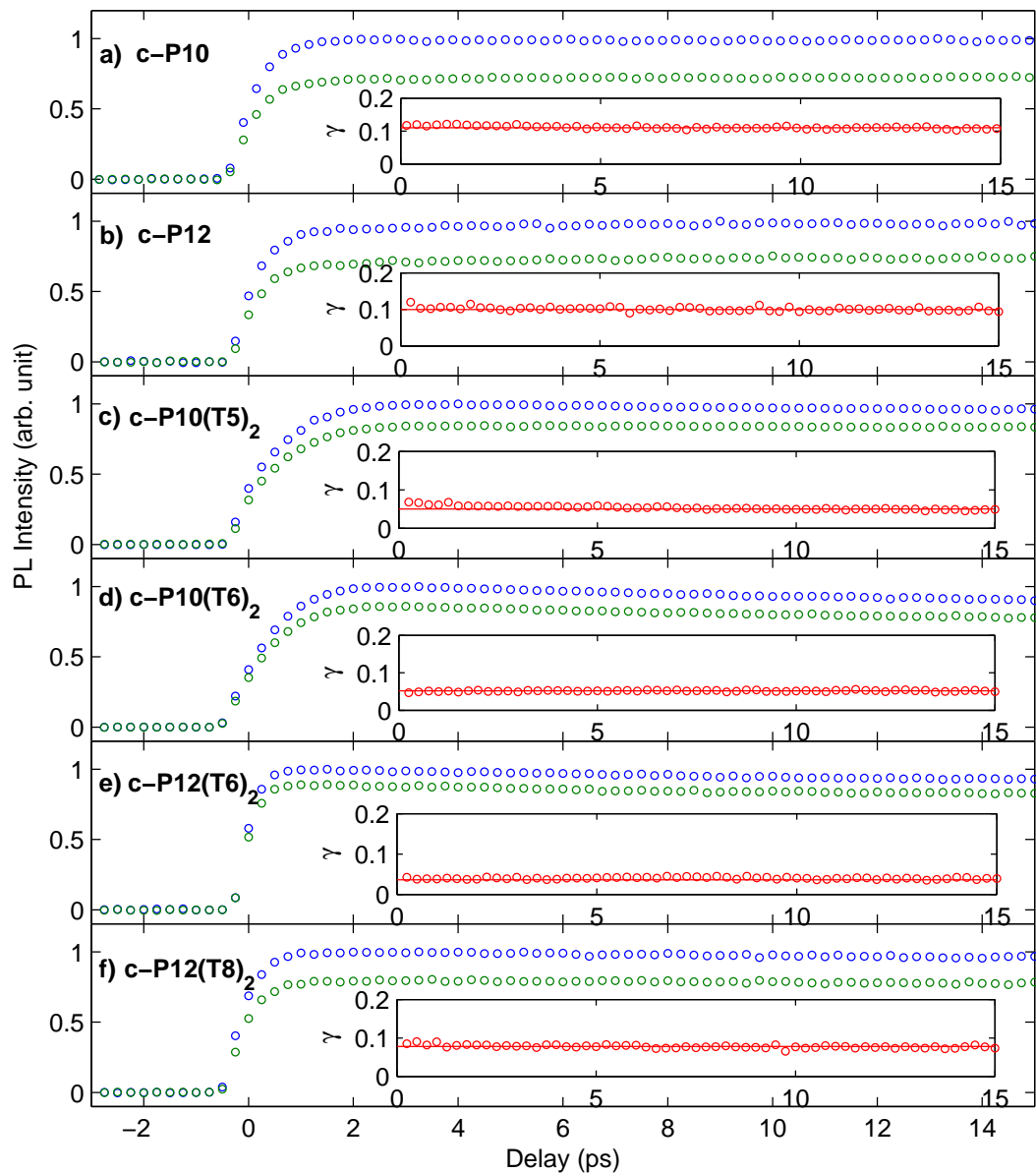


Figure S3: PL emission transients for (a) *c*-P10, (b) *c*-P12 in toluene/1% pyridine excited at 780 nm and (c) *c*-P10·(T5)<sub>2</sub>, (d) *c*-P10·(T6)<sub>2</sub>, (e) *c*-P12·(T6)<sub>2</sub>, (f) *c*-P12·(T8)<sub>2</sub> in toluene solution excited at 820 nm. The PL was detected at the peak emission wavelength. Samples were excited with light polarized either parallel ( $I_{\parallel}$ , blue) or perpendicular ( $I_{\perp}$ , green) to the detection polarization. Insets show the PL anisotropy dynamics obtained from  $\gamma = (I_{\parallel} - I_{\perp}) / (I_{\parallel} + 2I_{\perp})$ , together with a straight-line fit.

## Anisotropy Modelling

A simple model is used to describe the porphyrin nanoring conformations and link these with the measured PL anisotropy values. As illustrated in Figure S4, porphyrin monomer units are assumed to form two smaller loops, each lying in one plane (corresponding to the template plane). The angle between the planes are taken to be the RMS values extracted from the *HyperChem* simulations described in the main manuscript. Further assumptions have been made: 1. The initially excited and the emitting states are discretized to extend over one monomer at a time. This is justified, because the observed anisotropy dynamics is static due to fast depolarization process ( $< 300$  fs) which suggests that all sites are excited and emit with similar probability. Hence the calculated anisotropy value based on averaged contributions from individual sites is not affected by delocalization length in such a circular arrangement; 2. The dipole moments are aligned tangentially to the circle which the porphyrins are forming; 3. Each monomer has equal probability of absorbing and emitting a photon.

The PL Anisotropy is then calculated using the equation:  $\gamma_s = \frac{1}{5}(3\langle \cos^2 \kappa \rangle - 1)$ , where  $\kappa$  denotes the angle between the dipole moments of the absorbing and emitting states. For excitation at each monomer site,  $\cos^2 \kappa$  with respect to any porphyrin unit on the ring is summed over and the average is taken.



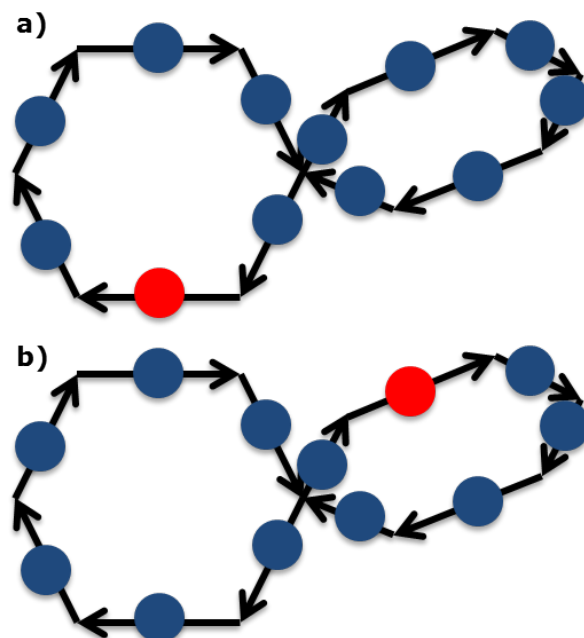


Figure S4: Oscillator distributions on nanorings assumed for PL anisotropy modelling: Circles denote porphyrin monomers and the arrows represent transition dipole moments. Porphyrin units are arranged in two smaller loops lying on two planes defined by the templates. (a) Initially excited state (red); (b) emitting state.

## Molecular Dynamics and PL Depolarization at 600 K

Molecular Dynamics simulations were carried out at a constant temperature of 600 K in time steps of 1 fs for a time window of 500 ps under the same conditions as the simulations at 300 K described in the main text. Twisting and bending angles  $\alpha$  and  $\beta$  were recorded and the results are summarized in Figure S5(a)-(d), with the root-mean-square (RMS) values listed in Table S1. A broader angle spread in the twisting angle  $\alpha$  is observed compared to the simulation results at 300 K, commensurate with what would be expected from the additional energy available. The calculated PL anisotropy results based on the molecular dynamics simulation at 600 K are listed in Table S1 and compared with experimental results. The PL anisotropy is not affected to a large extent and exhibits similar trends to simulations at 300 K.

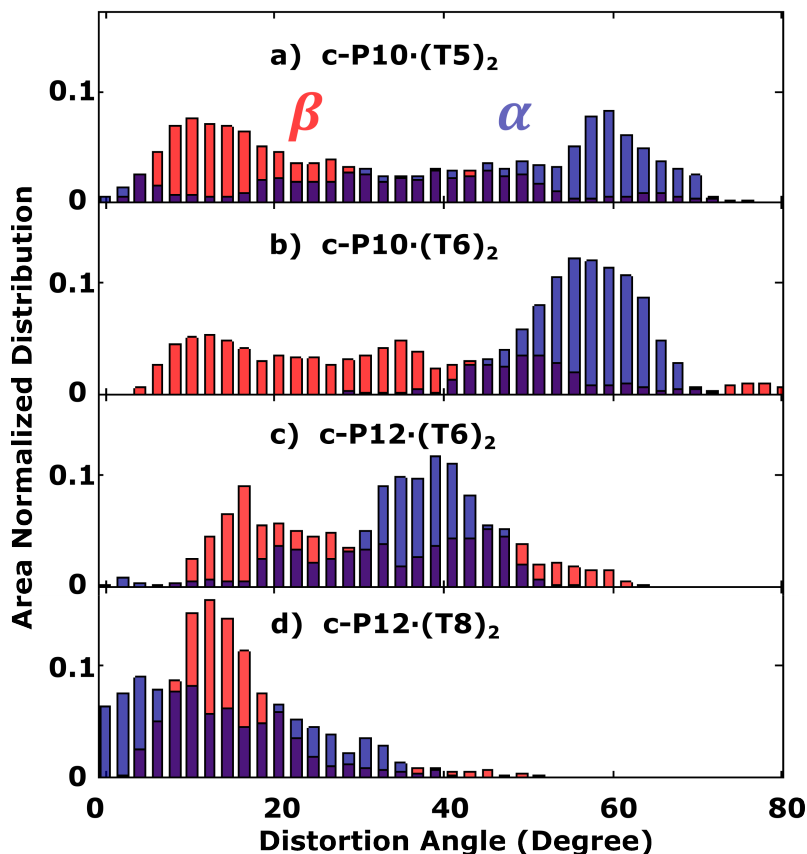


Figure S5: Area normalized histogram of twisting angle  $\alpha$  (blue) and bending angle  $\beta$  (red) for (a)  $c\text{-P10}\cdot(\text{T5})_2$ , (b)  $c\text{-P10}\cdot(\text{T6})_2$ , (c)  $c\text{-P12}\cdot(\text{T6})_2$ , (d)  $c\text{-P12}\cdot(\text{T8})_2$ . Molecular dynamics simulation carried out using *HyperChem* at 600 K for 500 ps, as described in detail in the text.

Table S1: Root-mean-squared values of the distortion angles  $\alpha$  (twisting) and  $\beta$  (bending) obtained for the templated rings from molecular dynamics simulation using *HyperChem* at 600 K. Using a simplified model based on the results from *HyperChem* as described in the main text, simulated anisotropy values  $\gamma_s$  are obtained.

Molecule	$\sqrt{\langle\alpha^2\rangle}$	$\sqrt{\langle\beta^2\rangle}$	$\gamma_s$
$c\text{-P10}\cdot(\text{T5})_2$	48°	30°	0.06
$c\text{-P10}\cdot(\text{T6})_2$	56°	39°	0.05
$c\text{-P12}\cdot(\text{T6})_2$	36°	34°	0.06
$c\text{-P12}\cdot(\text{T8})_2$	17°	18°	0.09